JMB

Probing Interactions within the Synaptic DNA-SfiI Complex by AFM Force Spectroscopy

Alexey V. Krasnoslobodtsev, Luda S. Shlyakhtenko and Yuri L. Lyubchenko*

Department of Pharmaceutical Sciences, University of Nebraska Medical Center, Omaha NE 68198, USA

SfiI belongs to a family of restriction enzymes that function as tetramers, binding two recognition regions for the DNA cleavage reaction. The SfiI protein is an attractive and convenient model for studying synaptic complexes between DNA and proteins capable of site-specific binding. The enzymatic action of SfiI has been very well characterized. However, the properties of the complex before the cleavage reaction are not clear. We used single-molecule force spectroscopy to analyze the strength of interactions within the SfiI–DNA complex. In these experiments, the stability of the synaptic complex formed by the enzyme and two DNA duplexes was probed in a series of approach–retraction cycles. In order to do this, one duplex was tethered to the surface and the other was tethered to the probe. The complex was formed by the protein present in the solution. An alternative setup, in which the protein was anchored to the surface, allowed us to probe the stability of the complex formed with only one duplex in the approach–retraction experiments, with the duplex immobilized at the probe tip. Both types of complexes are characterized by similar rupture forces. The stability of the complex was determined by measuring the dependence of rupture forces on force loading rates (dynamic force spectroscopy) and the results suggest that the dissociation reaction of the SfiI–DNA complex has a single energy barrier along the dissociation path. Dynamic force spectroscopy was instrumental in revealing the role of the 5 bp spacer region within the palindromic recognition site on DNA–SfiI in the stability of the complex. The data show that, although the change of non-specific sequence does not alter the position of the activation barrier, it changes values of the off rates significantly.

© 2006 Elsevier Ltd. All rights reserved.

Keywords: synaptic complex; force spectroscopy; protein–DNA interactions; AFM; site-specific recognition

*Corresponding author

Introduction

The protein SfiI is a member of subgroup IIF restriction enzymes and functions as a homotetramer.[1] It recognizes and binds specifically two DNA duplexes containing 13 bp recognition sites 5′-GGCCNNNN↓NGGCC-3′ (N is any base; the arrow indicates the cleavage position), in which two tetranucleotide-specific sequences are separated by a non-specific 5 bp region. Interestingly, although

the sequence of this internal 5 bp spacer is not critical for the site-specific recognition, it modulates the rate of the cleavage reaction.[2] Magnesium is required as a cofactor for SfiI to cleave DNA; however, in the presence of Ca^{2+} instead of Mg^{2+}, SfiI forms a stable complex without DNA cleavage.[3] This makes SfiI very convenient for studying the formation of a synaptic complex, and its characteristic features such as site-specific recognition and binding.

SfiI enzymatic activity has been very well characterized.[4] However, structural data for this system were not available until recently. We used atomic force microscopy (AFM) to resolve the arrangement of the DNA duplexes within the SfiI–DNA complex.[5] This study showed that the two DNA recognition regions remain almost straight and are crossed at an

angle of 60° with respect to each other. Simultaneously published crystallographic data for the SfiI-DNA complex[6] were in perfect agreement with the AFM results. According to the crystallographic data, each SfiI monomer binds a 4 bp (GGCC) sequence, so that the SfiI dimeric unit can bind only one duplex with the entire 13 bp recognition site. SfiI protein has been shown to exist as a tetramer in solution.[7] The SfiI tetramer, therefore, can form either a synaptic complex with two duplexes or a pre-synaptic complex where only one duplex is bound to the protein. The central part of the entire DNA-binding region (NNNN$^{\downarrow}$N) is not essential for binding specificity, as the protein has no direct contact with the bases inside the spacer. Naturally occurring sequences are cleaved by SfiI at different rates.[7] The nature of this effect is still not fully understood; however, the flexibility of the spacer was discussed as the most probable cause of the effect.[2,6]

Despite the fact that SfiI enzyme is well characterized functionally,[1,4,7–12] there are no data available about the stability of the complex or the kinetics of the complex dissociation. The availability of these data is important for understanding the mechanisms of the complex formation and the way the recognition process proceeds. In this study, we applied single molecule force spectroscopy to further characterize properties of the SfiI–DNA complex. Single molecule force spectroscopy has recently evolved into a powerful method to measure strength of intermolecular interactions on a single-molecule level.[13–16] Also, the information obtained by the dynamic force spectroscopy (DFS), can be related to thermodynamic and kinetic parameters of the donor–acceptor system measured in bulk.[17–20] Such experiments often require covalent attachment of the target molecules, and we have recently developed and tested the surface chemistry, which allows simple and reliable anchoring of target molecules with free thiol groups to a surface.[21]

We used single-molecule force spectroscopy to measure the stability of the synaptic SfiI–DNA complex. We used DFS to reveal the energy landscape for the SfiI–DNA complex dissociation, which is not accessible by any other technique. The DFS data showed that the dissociation reaction of the SfiI–DNA complex is defined by a single energy barrier. The dissociation rate values were found to be quite high, suggesting a dynamic nature of complexes for the studied DNA substrates. The contribution of the non-specific spacer in the DNA recognition site to the stability of the complex was studied, and the role of this sequence in the complex formation is discussed.

Results

Experimental design

Double-stranded 40 bp oligonucleotides were designed to contain a 13 bp recognition sequence (5′-GGCCNNNNNGGCC-3′) near the 3′ end. The thiol group modification at the 5′ end provided a means for covalent anchoring of the duplex to surfaces. The thiol group was attached *via* flexible single-stranded DNA, using either a dT_{10} or a dT_{50} linker to reduce potential stereochemical complications for the formation of the complex of SfiI with the tethered DNA duplex. The mica and the AFM probe tip surfaces were functionalized using the maleimide surface immobilization chemistry (see Materials and Methods).[21]

Figure 1 illustrates the experimental setup used for studying synaptic complexes. With no SfiI protein present in the solution, the probing of interactions between the probe tip and the surface produced no rupture event and only short-range adhesion forces were observed (Figure 1(a)). Adding the SfiI protein resulted in the formation of a complex between protein and DNA duplexes after the probe tip approached the surface (Figure 1(b)). The complex is probed by applying a pulling force to the formed complex (Figure 1(c)). Note that, due to the symmetry of the complex, both duplexes can dissociate upon
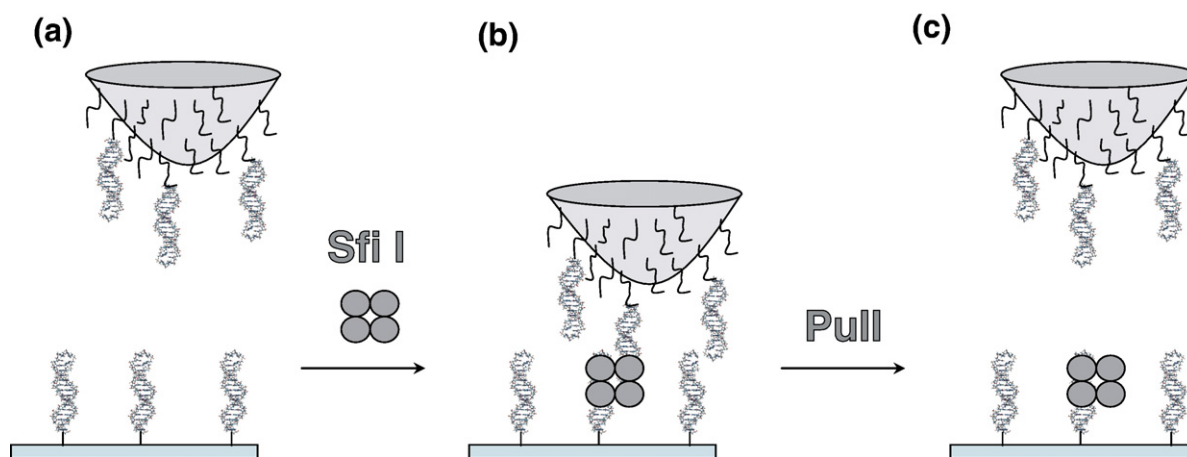
Figure 1. A representation of the experiment for studying synaptic SfiI–DNA complexes. (a) Oligoduplexes were covalently attached to the AFM probe tip and the mica surface. (b) The solution of SfiI in buffer was added between the probe tip and the surface, resulting in the formation of a synaptic complex after the tip of the probe approaches the surface. (c) Application of a pulling force results in rupture of the complex.

applying the force. Only one option (dissociation of the left duplex) is shown in the Figure for simplicity.

Figure 2 shows our approach for probing the stability of the pre-synaptic SfiI–DNA complex. SfiI protein was covalently anchored to the mica surface *via* the –SH group of cysteine residue of SfiI. There is a unique cysteine residue near the C terminus of the protein (230th out of 269), and according to the crystallographic data, this part of the protein is not involved in the recognition site of the protein.[6] The interactions between DNA and the protein in the pre-synaptic complex were probed with the DNA oligonucleotide attached to the AFM probe tip (Figure 2(a)).

Force spectroscopy study of synaptic SfiI-DNA complex

A typical force-distance curve obtained using the experimental setup for studying the synaptic complex represented by Figure 1(a)–(c) is shown in Figure 3. An adhesive peak at the beginning of the force curve (section 1 of the force curve) is accom-

panied by a force extension curve (section 2) corresponding to the stretching of polymer linkers,[22] followed by a rupture event (section 3).[21] We interpret the magnitude of this force change as the force required to break the interactions between DNA and SfiI protein within the complex. This assumption was supported by control experiments in which the pulling was performed with a large excess of free duplex in solution. Binding of free duplexes to SfiI prevents the formation of the complex during the approach of the probe tip to the surface and thus no rupture event is detected. The rupture effect is not observed if EDTA is added to the protein solution, due to chelation of the divalent cations that are critical for formation of the SfiI–DNA complex. These control experiments provide strong evidence to support our interpretation of a rupture event as breaking specific interactions between SfiI and DNA.

The forces required to break the synaptic complex were systematically analyzed and compiled in histogram. The inset in Figure 3 shows such a his-
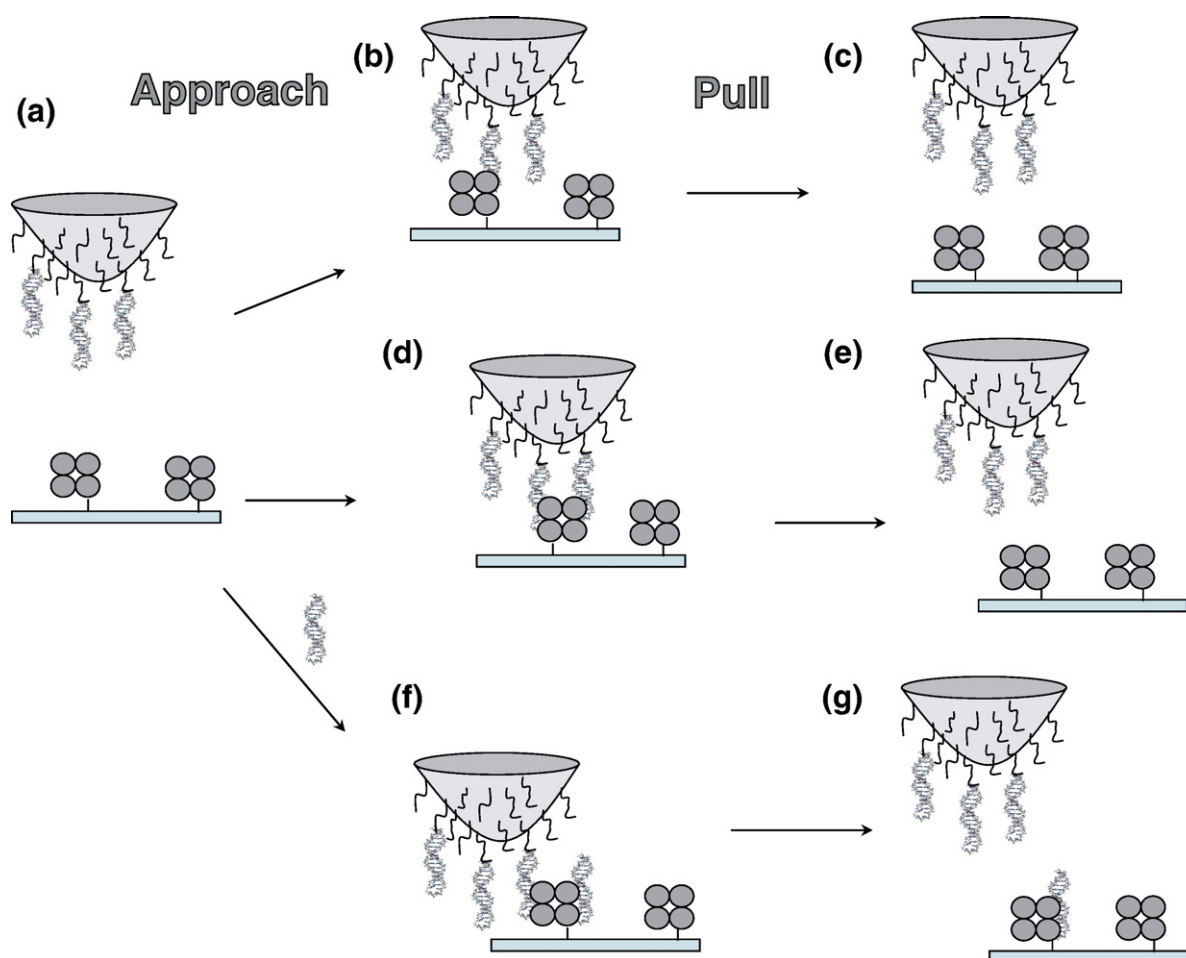
Figure 2. A representation of the experiment with protein immobilization for studying presynaptic SfiI–DNA complexes. (a) The AFM probe tip was modified with oligoduplexes and SfiI was immobilized on the surface. (b) The tip of the probe approaches the surface to form the complex. (c) Application of a pulling force results in rupture of the presynaptic complex. (d) and (e) A high concentration of target molecules results in rupture of multiple contacts. (f) and (g) Addition of free DNA duplex to the solution increases the probability of a single complex rupture due to blocking the SfiI active sites.
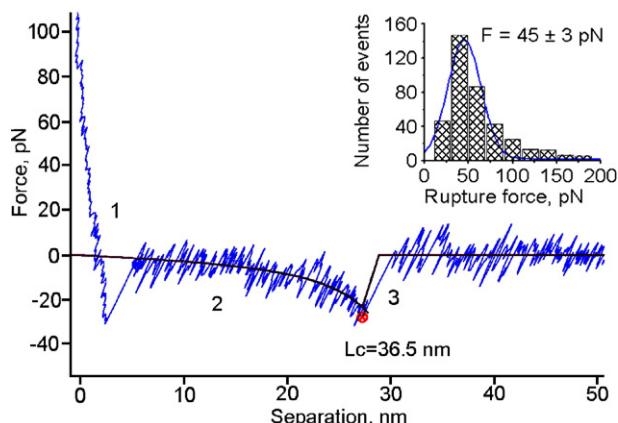
Figure 3. A typical force–distance curve obtained for the interactions between SfiI and the DNA oligonucleotide. (1) The start of retraction of the probe tip from the surface, the force curve in this region reflects the non-specific adhesion forces between the surface and the tip of the probe. (2) The region is indicative of polymer linker stretching, this portion of the curve is fit with a worm-like chain approximation (continuous red line). (3) The abrupt jump in the force curve is typical of rupture of a specific bond. The inset shows the rupture force histogram obtained for the synaptic complex at a retraction velocity of 150 nm/s (~9.5 nN/s apparent loading rate).

togram for the data obtained from analysis of complex rupture forces at a pulling velocity of 150 nm/s (9.5 nN/s apparent loading rate). The Gaussian fit to the distribution provides the most probable rupture force of 45($\pm$3) pN.

Additional evidence to support the interpretation of the force spectroscopy data as the force-induced dissociation of the SfiI–DNA complex comes from the measurements of the linker extension from zero distance to the position of the complex rupture in a force–distance curve. As shown in Figure 3, the contour length of the extended linker determined from the approximation of the elastic part by the worm-like-chain (WLC) model (see Materials and Methods) is 36.5 nm. This value is in good agreement with expected extension of the linkers for the system (~36 nm). The expected rupture length was estimated by adding together the length of the maleimide silatrane linker containing five polyethylene glycol monomeric units in all-*trans* conformation (3.3 nm),[21] the size of the SfiI itself (6.8 nm),[6] the extension of the $(dT)_{10}$ spacer, and the part of the oligonucleotide that is not complexed with the protein, assuming 0.34 nm per base-pair.

We performed experiments with linkers of various lengths. The results of measurement of the rupture length for 500 various rupture events for different linkers are shown in Figure 4(a)–(c). The most probable rupture lengths are the maxima of the distribution obtained as mean values from Gaussian fit. The rupture lengths are equal to 39 nm, 53 nm and 71 nm for $(dT)_{10}$ (Figure 4(a)), $(dT)_{50}$ (Figure 4(b)), and PEG (Figure 4(c)) linkers, respectively. These values are in good agreement with the expected values, which are equal to 36 nm, 50 nm and 61 nm

for $(dT)_{10}$, $(dT)_{50}$ and PEG linkers, respectively, calculated as described above. The increased width of the distribution for the experiments with long PEG linker (histogram c in Figure 4) is attributed to the length heterogeneity of commercially available polyethylene glycol polymers (3400 g/mol) ranging between 20 nm and 30 nm.[23]

AFM study of the SfiI–DNA complex; the SfiI immobilization approach

An alternative strategy depicted in Figure 2(a) was used to investigate the pre-synaptic SfiI–DNA complex. In this approach, the enzyme was covalently attached to the maleimide-functionalized mica surface *via* the only cysteine residue of the protein, and the interactions were probed with the oligonucleotide anchored to the tip of the AFM probe. A representative force–distance curve obtained using this experimental setup is shown in Figure 5. This curve is similar to that obtained for the synaptic complex (Figure 3) and has characteristic rupture event, illustrating that the complex formation being studied is between a single DNA duplex and the enzyme. Only force curves with single rupture events like the one shown in Figure 5 were analyzed. The results of the rupture force measurements for a large set of such curves are summarized as a histogram in the inset in Figure 5. The most probable rupture force for the dissociation of the DNA–SfiI complex is 80($\pm$5) pN at a pulling velocity of 150 nm/s (9.5 nN/s apparent loading rate), that is almost twice the rupture force value obtained for the synaptic complex (Figure 3).
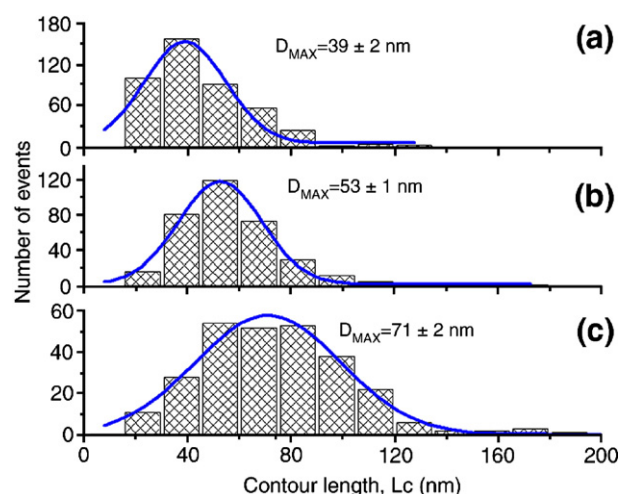
Figure 4. Distributions of contour lengths obtained from WLC fitting for different linkers. (a) The 10 bp poly(T) linker for the oligonucleotide on the probe tip and on the surface, producing 36 nm of contour length. (b) The 50 bp poly(T) linker for the oligonucleotide on the probe tip and the 10 bp poly(T) linker for the oligonucleotide on the surface (50 nm). (c) The 10 bp poly(T) + PEG (3400 g/mol) linker for the oligonucleotide on the probe tip and the 10 bp poly(T) linker for the oligonucleotide on the surface (61($\pm$5) nm).
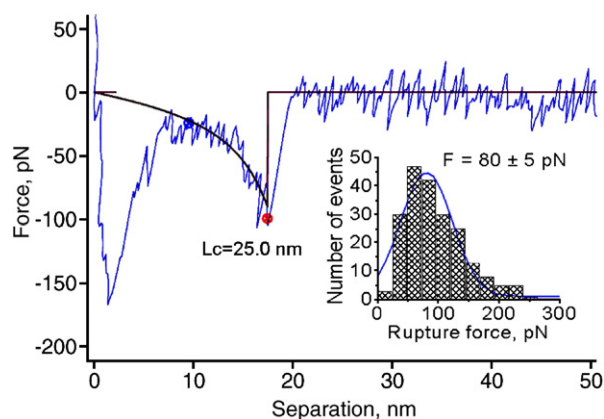
Figure 5. A typical force–distance curve for the interactions between the DNA oligonucleotide and the surface-immobilized SfiI. The inset shows the rupture force histogram obtained for the pre-synaptic complex at a retraction velocity of 150 nm/s (~9.5 nN/s apparent loading rate).

We carried out control experiments in which probing of immobilized SfiI by the tip were performed in the presence of DNA duplex capable of binding SfiI. The motivation for these experiments was that the synaptic complex, in addition to the pre-synaptic complex, can be formed and probed as well. Free DNA duplex can bind to the tethered enzyme occupying one of the binding sites, so only one DNA-binding site remains available for the probing: this possibility is illustrated in Figure 2(g) and (f). The experimental data obtained at a pulling velocity of 150 nm/s (~6.5 nN/s apparent loading rate) are shown as histograms in Figure 6(a). Two distinct peaks with mean values 33 pN and 63 pN are clearly resolved, suggesting the formation of two types of complexes probed by the AFM pulling experiments. The extensions of the linker were measured from the force curves, and the results are summarized in Figure 6(b). The experimental value of the rupture length was determined as the maximum of the Gaussian fit to the statistical histogram measured for over 1000 rupture events. The experimental value of 31 nm is very close to the expected rupture length for covalently attached SfiI (27 nm), supporting the interpretation that specific DNA–SfiI interactions were detected.

A peak with a low rupture force value, 33 pN, appears in these experiments, suggesting that, in addition to pre-synaptic complex, we were able to detect the formation of the synaptic complex. The lower value for the rupture force is explained by the slower loading rate used in these experiments (see the dependence of the rupture force on the loading rate below). Therefore, the peak with a high rupture force corresponds to probing pre-synaptic complexes, suggesting that the rupture forces for these complexes are considerably greater than those for the synaptic complex. However, we have to consider an alternative model in which two hanging DNA duplexes form a complex with the enzyme (Figure

2(d)), so the dissociation of such a complex (Figure 2(e)) requires a large rupture force. Although we have deliberately chosen to analyze only force curves with apparent single rupture events, one can never eliminate the possibility of double contact rupture in AFM experiments. To distinguish between the two aforementioned possibilities, we have performed an experiment with a lower (tenfold) surface concentration of DNA duplexes on the probe; and the results are shown in Figure 7. Experiments in the absence of the duplex in solution provide forces spanning over a broad range, so the distribution can be resolved into two Gaussians (blue histogram in Figure 7). The peak for low forces corresponds to a value of 38 pN, and the second peak is centered around 88 pN. After addition of free DNA to the solution, the large forces disappear, so the histogram is approximated by one Gaussian with a peak value of 35 pN (red histogram in Figure 7). These are the events combining synaptic and pre-synaptic complexes that we are unable to resolve, suggesting that the stability of these two complexes is quite similar. It should be noted that the tenfold decrease of the concentration of the duplex in the reaction mixture for the probe tip functionalization did not remove the probability of double rupture events. This effect could be due to a relatively short polymer tether, which may not provide enough flexibility, because the use of longer linker ((dT)$_{50}$) revealed the first peak at higher concentrations of DNA (data not shown). Thus, the data obtained are in favor of the second model, suggesting that probing of immobilized enzyme leads to the formation of pre-synaptic complex by one hanging
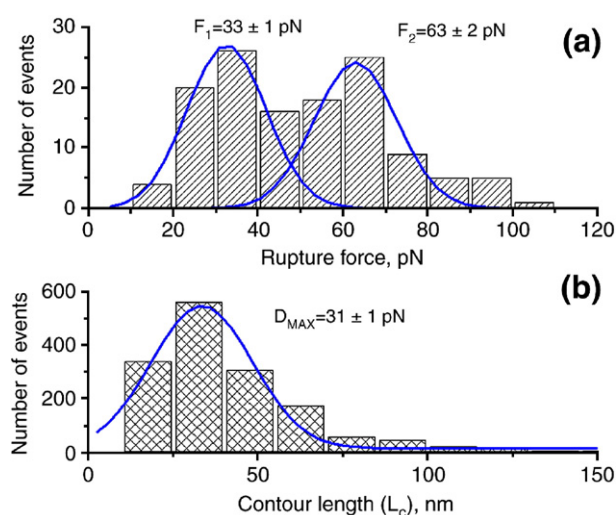
Figure 6. (a) Rupture of SfiI–DNA complexes in the experiments with covalently attached protein and free oligoduplexes in solution (GGCCTCGAGGGCC–recognition sequence) at a retraction velocity of 150 nm/s (~6.5 nN/s apparent loading rate). Two distinct populations of forces are evident (see the text for details). (b) Distributions of contour lengths obtained from worm-like-chain fitting in the experimental setup with surface-immobilized SfiI and oligoduplex with (dT)$_{10}$ linker on the probe tip (27 nm).
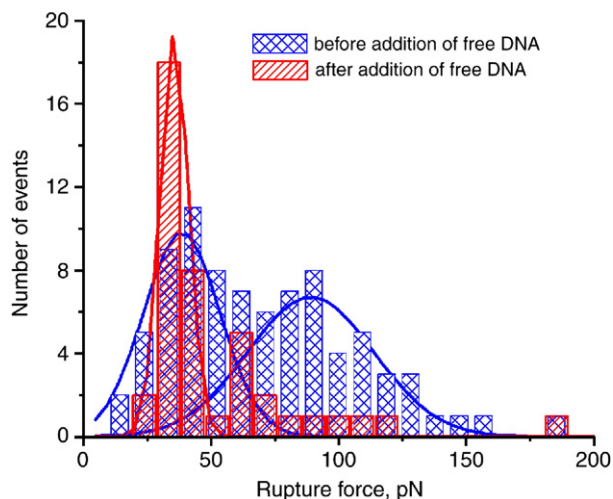
Figure 7. The rupture force distribution at low concentration of DNA on the probe tip. Two force populations are observed (blue histogram): the first peak corresponds to single complex rupture, the second peak corresponds to the situation when two complexes are ruptured simultaneously. Addition of free DNA duplex to the solution eliminated the possibility of double contact formation (red histogram).

duplex and a synaptic complex formed by two immobilized DNA duplexes.

Dynamic force spectroscopy study

In order to characterize the properties of the SfiI–DNA complex at conditions approaching the equilibrium, we applied the DFS by performing pulling experiments at various loading rates.[17,24] The strength of interactions within SfiI–DNA complexes was tested over a wide range of loading rates. The histograms of forces collected for each experi-
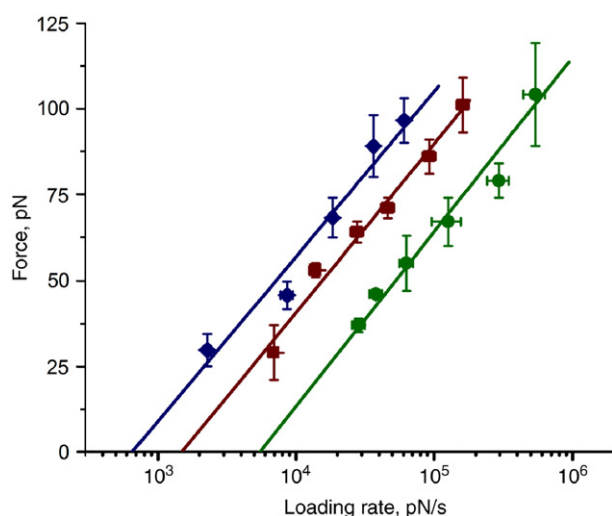
Figure 8. Dynamic force spectra of SfiI–DNA complexes for three spacer sequences: TCGAG, blue; AAACA, red; AAAAA, green.

ment were approximated by Gaussian distributions, and the values corresponding to the maxima for each distribution were plotted against the logarithm of apparent loading rate. Figure 8 (blue symbols and line) shows such a plot, which reveals that the data are fit with linear plot. According to equation (1):

$$F_R = \frac{k_B T}{x_\beta} \ln\left(\frac{v x_\beta}{k_{off} k_B T}\right) \qquad (1)$$

the slope of the linear fit allows us to determine the position of the activation energy barrier along the direction of applied force.[25] The value of the dissociation rate k_{off} was obtained by extrapolating the experimental data to zero rupture force. These data, along with the x_β values, are given in Table 1. It should be noted that the dependence of the rupture force on the loading rate was very similar for both pre-synaptic and synaptic SfiI–DNA complexes, thus providing similar values of x_β and k_{off}.

Spacer sequence dependence

The SfiI enzyme recognizes a palindromic sequence of the DNA duplex (5′-GGCCNNNN$^\downarrow$NGG-CC-3′). The central part of the entire DNA-binding region, a 5 bp non-specific spacer (NNNN$^\downarrow$N) is not essential for binding specificity,[26] and according to the crystallographic data, the protein has no direct contact with the DNA bases inside the spacer.[6] However, this 5 bp central sequence affects the enzymatic activity of the SfiI endonuclease.[2] Naturally occurring sequences are cleaved by SfiI at different rates.[7] To gain insight into the role of this part of the DNA cognate region in the complex stability, we performed force spectroscopy measurements with three different central 5 bp sequences. Previous studies on SfiI activity have used several different sequences.[2] Among them AAAAA and AAACA were used to reveal the effect of rigidity of the DNA spacer structure on the activity of the enzyme. The former sequence consists of adenine only, thus imparting rigidity to the DNA structure. The latter sequence has an oligo(A) sequence disrupted by a single C that was used to clarify the effect of a single-base substitution. The enzymatic activity of the SfiI was reported to increase by a factor of 5 upon a change from AAAAA to AAACA.[2] We also compared these two sequences with TCGAG, a spacer of a random sequence. The complexes formed by each duplex

Table 1. Experimental values of k_{off} and x_β for the SfiI–DNA complex obtained using dynamic force spectroscopy

Recognition sequence	k_{off} (s^{-1})	$x\beta$ (Å)
5′GGCCT CGA^GGGCC CCGGA^GCT CCCGG 3′	38(8)	1.8(0.2)
5′GGCCA AAC^AGGGCC CCGGT^TTG TCCCGG 3′	70(11)	1.9(0.1)
5′GGCCA AAA^AGGCC CCGGT^TT T TCCGG 3′	248(79)	1.9(0.2)

Standard errors of the experimentally determined values are given in parentheses.

design were studied by DFS to obtain kinetic parameters for the complexes as described above. The results of the DFS analysis are shown in Figure 8. For each complex, the data points for the most probable rupture forces fall on straight lines that are different for each sequence. If the slopes for these linear plots are quite similar, the lines shift relative to each other, suggesting that the linker sequence influences dissociation rates of the complex. The effect is rather strong, so that the stability of the complexes for the sequences analyzed varies by an order of magnitude. For example, replacement of the spacer sequence from 3′-TCGAG-5′ to 3′-AAAAA-5′ results in the increase of dissociation rate from 38 s^{-1} to 248 s^{-1}. Table 1 summarizes dissociation rates, k_{off}, as well as the energy barrier positions, x_β, for all three non-specific spacer sequences (NNNNN).

Discussion

Dynamic force measurements using our experimental strategies permitted us to reconstruct the energy landscape of the dissociation reaction of the SfiI–DNA complex, which is not accessible by any of the other techniques applied to this system so far. The data points for the most probable unbinding force fall on a single linear plot, suggesting that the dissociation path of the complexes has a single barrier on the energy landscape. Note that single barrier mechanisms were observed for DNA–protein systems such as restriction enzymes BsoBI, XhoI[27] and a binding domain of PhoR transcription activator.[28] Our data obtained for the range of forces starting with as low as 20 pN (the lowest values for typical AFM experiments) comply with the single-barrier model. Another parameter that can be determined from the DFS analysis is the height of the energy barrier, $\Delta G^{\#}$, which determines the dissociation rate and, therefore, the lifetime of a complex according to the following equation:[29]

$$k_{off}^0 = \frac{k_B T}{h} \exp\left(-\frac{\Delta G^{\#}}{k_B T}\right) \qquad (2)$$

The analyses performed for the three duplexes that differed in the spacer sequence provided the following $\Delta G^{\#}$ values: 15.5 kcal/mol for 3′-TCGAG-5′, 14.4 kcal/mol for 3′-AAAAA-5′, and 15.1 kcal/mol for the intermediately stable 3′- AAACA-5′ sequence. These activation energy differences translated to a substantial difference in the dissociation off-rates (Table 1), which is the major effect of the 5 bp spacer sequence on the complex stability.

For the data analysis, we used the plot of most probable rupture forces obtained from the Gaussian fit of force histograms *versus* the values of the apparent loading rate (the retraction velocity multiplied by the spring constant of the AFM probe). This treatment of the data assumes that the force loading rate dF/dt is constant. However, this assumption may not be valid if a flexible linker is used for tethering the molecules. The utilization of the

polymer linkers reduces the ambiguity of data analysis. First, the specific rupture events are moved away from the strong non-specific adhesion peak. Second, it greatly reduces the probability of measuring multiple interactions between the probe tip and the surface. A traditional tether is PEG, a flexible polymer with relatively small persistence length P (~0.3 nm) and it was shown that the spring constant of such a linker can contribute to the non-linearity of the dependence of applied force on the separation.[30] In our experiments, we used a linker consisting primarily of single-stranded poly(dT). This polymer is considerably stiffer than PEG and is characterized at the ionic conditions used at the persistence length of ~3 nm.[31] The spring constants of polymeric molecules fall as $(P)^{-2}$;[32] therefore, an anticipated spring constant for (dT)$_n$ linkers is 100 times less than that of PEG, suggesting that this polymer extends at very low applied forces. Single-stranded DNA with no secondary structure extends at forces of ~4 pN,[33] which is considerably less than the minimal 13 pN noise level for the AFM cantilevers used in this work.[34] The linker used in this study is complex, containing short polyethyleneglycol (five monomeric units), single-stranded poly(dT) ((dT)$_{10}$ and (dT)$_{50}$) and double-stranded DNA (part of the duplex that is not involved in complex formation with SfiI). To test that the estimates are valid, we performed experiments with (dT)$_n$ linkers of two different lengths, ten and 50 monomer units. The results in Supplementary Data Figure S3 show that, despite the fivefold difference in length between (dT)$_{10}$ and (dT)$_{50}$ linkers, they did not display substantial difference in the dependence of the rupture forces on the apparent loading rate. This result characterizes the poly(dT) linker as a very good candidate for the force spectroscopy measurements when tethering *via* flexible linker is required.

There are two common methods used in the literature for data analysis and obtaining energy barrier position x_β and off-rate values k_{off}. One method uses the dependence of rupture force on probe velocity (apparent loading rate).[30,35–38] An alternative approach has been proposed that overcomes the deficit of the assumption of linear force/time dependence used in derivation of equation (1). This approach uses the so-called effective loading rate instead of the apparent loading rate.[13,14,39,40] The effective loading rate is determined experimentally from the slope of the force *versus* time immediately before the rupture point (as shown in Supplementary Data Figure S1). We have compared both methods of data analysis for one of the sequences (GGCCTCGAGGGCC). The comparison of the rupture force dependence on apparent *versus* effective loading rate reveals that the two methods provide different values of the definable parameters. The energy barrier position is slightly underestimated and the off-rate is overestimated by factor of 2.7 when effective loading rate was used (Supplementary Data Figure S2) as compared to use of the apparent loading rate.

We have found that the central 5 bp region in the recognition site sequences (5′-GGCCNNNN$\downarrow$NGG-CC-3′) between specific regions (GGCC) influences the stability of the SfiI–DNA complex. The recognition sequence with a TCGAG linker resulted in the formation of the most stable complex with $k_{off} = 38$ s^{-1}, while the spacer sequence AAAAA produced the least stable complex, with a large value of $k_{off} = 248$ s^{-1} (Table 1). Disruption of the run of consecutive adenine bases by a single cytosine base in the middle gives rise to a more flexible linker; as a result, a smaller value of k_{off} of 70 s^{-1} was measured. These findings are in line with the data on the spacer effect on SfiI catalytic activity. For example, SfiI cleaves GGCCAAA-CAGGCC about five times faster than the spacer sequence containing only adenine (GGCCAAAA-AGGCC).[2] A hierarchy of the non-specific 5 bp spacer sequence has been related to the flexibility of the spacer.[2] DNA sequences that contain an A-tract with ≥4 consecutive adenine bases are known to be rigid.[41] Indeed, according to the crystallographic data, DNA is slightly bent;[6] therefore, DNA with more flexible spacers should be better substrates for SfiI enzymatic action.[2] The same tendency of the sequence influence on the cleavage rates and complex dissociation rates permits us to conclude that there is an intimate relation between SfiI enzymatic activity and stability of the SfiI-DNA complex.

In principle, the SfiI–DNA complex can dissociate by different pathways under applied external force, breaking the DNA–protein contacts or possibly rupture of the protein tetramer. What is the weakest link? There are two major indirect pieces of evidence supporting the hypothesis that the DNA–protein contacts are broken upon the complex dissociation. First, if the protein–protein contacts were the weakest link, after the first pulling, the protein would remain bound to the tip of the probe. Therefore, the formation of the complex upon the second approach cycle would be unsuccessful until the protein dissociates from the probe tip. The delay would be essential in experiments with fast pulling rates. We did not notice such delays. Second, different spacer sequences produce different off-rates. According to the crystallographic data, there is no direct contact of the spacer with the protein and thus the effect of this sequence on the protein tetramer stability should be negligible. However, the difference in the values of the off-rates of almost one order of magnitude for various spacer sequences suggests substantial effect of the nature of the spacer, indicating that the bonds between DNA and SfiI are ruptured rather than protein–protein contacts.

The results on the off-rate measurements for the SfiI–DNA complex suggest that protein dissociates from the DNA template relatively fast with a characteristic time of ~30 ms. At the same time, AFM topography data show that the synaptic complex is quite stable; for instance, a high yield of complexes is observed at almost equimolar protein/DNA ratios.[5] One may suggest that the high off-rate values were obtained due to the extrapolation from relatively high loading rates typically used in the AFM experiments. For example, the use of a biomembrane force probe capable of measuring small forces for biotin–streptavidin complexes revealed a component in the force *versus* loading rate dependence with a small slope undetectable by AFM.[17] However, our recent measurements of the off-rate are constant with the use of the fluorescence correlation spectroscopy approach, provided the dissociation time of 9 ms, which is similar to the time range for the values obtained from the DFS experiments. These data suggest that the highly dynamic behavior of the SfiI–DNA complexes is a characteristic feature of this system rather than an artefact of the DFS technique.

To reconcile all observations, we propose the following model for the SfiI–DNA complex: The protein forms a dynamic complex in which it dissociates transiently from the DNA, but does it in such a way that it remains in close proximity to the recognition site. For example, the protein dissociates from one half of its discontinuous recognition sequence, but remains bound to another half. It binds again to the site, but may leave the second half of the recognition region. In other words, the DNA helix behaves as a roller swing that intermittently makes contacts with one or another DNA-binding site. The stiffer the spacer between these regions, the shorter the complex lifetime. Indeed, according to the crystallographic data, DNA is bent between the two GGCC-specific recognition regions; therefore, stiff duplexes between the binding sites should decrease the complex stability. This is exactly what we observed in the experiments with an AAAAA tract as the spacer, which has greater stiffness compared to the other tested sequences. Direct experiments are needed to test this model and these are in progress.

The synaptic SfiI–DNA complex has all of the features characteristic for the site-specific DNA recombination complexes formed by various proteins. Interaction of these proteins with DNA should be dynamic to facilitate accomplishing their major function of cutting and rearranging DNA molecules. Therefore, the approaches used here will be able to analyze such dynamic systems and provide a quantitative characterization of the biologically important nucleoprotein complexes.

Materials and Methods

Preparation of oligonucleotides

DNA oligonucleotides with flexible single-stranded poly(T) linker (either 10 bp or 50 bp), containing 13 bp recognition site (3′-GGCCNNNNNGGCC-5′) and thiol modification at the 5′ end were purchased from Integrated DNA Technologies, Inc. as single-stranded

complements. The oligonucleotides were dissolved in double-distilled water and 20 μl aliquots were stored at −80 °C. Complementary oligonucleotides were annealed by heating to 98 °C, followed by slow cooling to room temperature. To reduce protected thiol groups of the oligonucleotides, the duplexes were treated with 10 mM Tris(2-carboxyethyl)phosphine (TCEP) hydrochloride in 10 mM Hepes (pH 7.0), 50 mM NaCl at 25 °C for 10 min.

Probe tip and surface modification

Silicon nitride (Si₃N₄) AFM probe tips were washed in ethanol by immersion for 30 min and then activated by UV treatment for 30 min. Activated probe tips and the freshly cleaved mica surface were treated with 167 μM maleimide-silatrane for 3 h followed by rinsing with double-distilled water. Maleimide-functionalized AFM probe tips and mica were incubated for 1 h in 10 μM and 80 μM double-stranded DNA, respectively. For covalent attachment of the SfiI protein, 8 nM protein (low BSA content, New England Biolabs) was treated with TCEP hydrochloride and then the maleimide-functionalized mica surface was incubated with this solution for 1 h. After washing with 10 mM Hepes (pH 7.0), 50 mM NaCl, unreacted maleimide was quenched with 10 mM β-mercaptoethanol in 10 mM Hepes (pH 7.0) for 10 min at room temperature. The modified probe tips and mica were washed with 10 mM Hepes (pH 7.0), 50 mM NaCl and stored in the same buffer.

AFM measurements

Force–distance measurements were performed in 10 mM Hepes (pH 7.0), 50 mM NaCl, 2 mM CaCl₂ at room temperature with the Molecular Force Probe 3D system (Asylum Research, Santa Barbara, CA). The ramp size was 300 nm with various loading rates. An application force was kept at a low value (100 pN). Silicon nitride cantilevers with nominal values of spring constants in the range of 0.04–0.07 N/m were used. Spring constants for each cantilever were obtained using a thermal method with the MFP-3D instrument. For control experiments, the SfiI protein was blocked by injection of a 2000-fold molar excess of DNA competitor. The approach and retraction velocities were 150 nm/s, except for a set of dynamic force measurements in which the approach velocity was fixed at 600 nm/s and the retraction velocity was varied between 50 nm/s and 10,000 nm/s, corresponding to the values of apparent loading rates (cantilever spring constant multiplied by retraction velocity) between 2.1×10^3 and 6.3×10^5 pN/s. The elastic response of a linker to applied force was analyzed by the Igor Pro 5.03 software package using WLC approximation. The effective loading rate values were determined from the slope of the force curve immediately before (~1 nm) the position of the rupture point. The end-to-end distances (contour lengths) were determined from the WLC fit of experimental force–distance curves. The most probable rupture force was obtained from the maximum of the Gaussian fit to the force distribution combined in a statistical histogram. Normally, the rupture forces of more than 500 rupture events were compiled in force distribution histograms. The maximum of the Gaussian fit to each histogram at any given loading rate defines the most probable rupture force, F_R, which is described by equation (1).[42]

Supplementary data

Supplementary data associated with this article can be found, in the online version, at doi:10.1016/j.jmb.2006.10.041

References

1. Nobbs, T. J., Szczelkun, M. D., Wentzell, L. M. & Halford, S. E. (1998). DNA excision by the Sfi I restriction endonuclease. *J. Mol. Biol.* **281**, 419–432.
2. Williams, S. A. & Halford, S. E. (2001). Sfii endonuclease activity is strongly influenced by the non-specific sequence in the middle of its recognition site. *Nucl. Acids Res.* **29**, 1476–1483.
3. Milsom, S. E., Halford, S. E., Embleton, M. L. & Szczelkun, M. D. (2001). Analysis of DNA looping interactions by type II restriction enzymes that require two copies of their recognition sites. *J. Mol. Biol.* **311**, 515–527.
4. Embleton, M. L., Vologodskii, A. V. & Halford, S. E. (2004). Dynamics of DNA loop capture by the Sfi I restriction endonuclease on supercoiled and relaxed DNA. *J. Mol. Biol.* **339**, 53–66.
5. Lushnikov, A. Y., Potaman, V. N., Oussatcheva, E. A., Sinden, R. R. & Lyubchenko, Y. L. (2006). DNA strand arrangement within the Sfi I-Dna complex: atomic force microscopy analysis. *Biochemistry*, **45**, 152–158.
6. Vanamee, E. S., Viadiu, H., Kucera, R., Dorner, L., Picone, S., Schildkraut, I. & Aggarwal, A. K. (2005). A view of consecutive binding events from structures of tetrameric endonuclease Sfi I bound to DNA. *EMBO J.* **24**, 4198–4208.
7. Wentzell, L. M., Nobbs, T. J. & Halford, S. E. (1995). The Sfi I restriction endonuclease makes a four-strand DNA break at two copies of its recognition sequence. *J. Mol. Biol.* **248**, 581–595.
8. Nobbs, T. J. & Halford, S. E. (1995). DNA cleavage at two recognition sites by the Sfi I restriction endonuclease: salt dependence of cis and trans interactions between distant DNA sites. *J. Mol. Biol.* **252**, 399–411.
9. Szczelkun, M. D. & Halford, S. E. (1996). Recombination by resolvase to analyse DNA communications by the Sfi I restriction endonuclease. *EMBO J.* **15**, 1460–1469.
10. Embleton, M. L., Williams, S. A., Watson, M. A. & Halford, S. E. (1999). Specificity from the synapsis of DNA elements by the Sfi I endonuclease. *J. Mol. Biol.* **289**, 785–797.
11. Wentzell, L. M. A. H. & Halford, S. E. (1998). DNA looping by the Sfi I restriction endonuclease. *J. Mol. Biol.* **281**, 433–444.
12. Williams, S. A. A. H. & Halford, S. E. (2002). Communications between catalytic sites in the protein-DNA synapse by the Sfii endonuclease. *J. Mol. Biol.* **318**, 387–394.
13. Kuhner, F., Costa, L. T., Bisch, P. M., Thalhammer, S.,

Heckl, W. M. & Gaub, H. E. (2004). LexA- DNA bond strength by single molecule force spectroscopy. *Biophys. J.* **87**, 2683–2690.

14. Schwesinger, F., Ros, R., Strunz, T., Anselmetti, D., Guntherodt, H. J., Honegger, A. *et al.* (2000). Unbinding forces of single antibody-antigen complexes correlate with their thermal dissociation rates. *Proc. Natl Acad. Sci. USA*, **97**, 9972–9977.

15. Ratto, T. V., Langry, K. C., Rudd, R. E., Balhorn, R. L., Allen, M. J. & Mcelfresh, M. W. (2004). Force spectroscopy of the double-tethered concanavalin-A mannose bond. *Biophys. J.* **86**, 2430–2437.

16. Hinterdorfer, P., Baumgartner, W., Gruber, H. J., Schilcher, K. & Schindler, H. (1996). Detection and localization of individual antibody-antigen recognition events by atomic force microscopy. *Proc. Natl Acad. Sci. USA*, **93**, 3477–3481.

17. Merkel, R., Nassoy, P., Leung, A., Ritchie, K. & Evans, E. (1999). Energy landscapes of receptor-ligand bonds explored with dynamic force spectroscopy. *Nature*, **397**, 50–53.

18. Dietz, H. & Rief, M. (2004). Exploring the energy landscape of GFP by single-molecule mechanical experiments. *Proc. Natl Acad. Sci. USA*, **101**, 16192–16197.

19. Yersin, A., Hirling, H., Steiner, P., Magnin, S., Regazzi, R., Huni, B. *et al.* (2003). Interactions between synaptic vesicle fusion proteins explored by atomic force microscopy. *Proc. Natl Acad. Sci. USA*, **100**, 8736–8741.

20. Cecconi, C., Shank, E. A., Bustamante, C. & Marqusee, S. (2005). Direct observation of the three-state folding of a single protein molecule. *Science*, **309**, 2057–2060.

21. Kransnoslobodtsev, A. V., Shlyakhtenko, L. S., Ukraintsev, E., Zaikova, T. O., Keana, J. F. & Lyubchenko, Y. L. (2005). Nanomedicine and protein misfolding diseases. *Nanomedicine*, **1**, 300–305.

22. Schumakovitch, I., Grange, W., Strunz, T., Bertoncini, P., Guntherodt, H. J. & Hegner, M. (2002). Temperature dependence of unbinding forces between complementary DNA strands. *Biophys. J.* **82**, 517–521.

23. Ratto, T. V. (2004). Force spectroscopy of the double-tethered concanavalin-A mannose bond. *Biophys. J.* **86**, 2430–2437.

24. Evans, E. & Williams, P. (2002). Dynamic force spectroscopy. I. Single Bonds. In *Physics of Bio-Molecules and Cells* (Flyvbjerg, H., Ormos, F. J. P. & David, F., eds), pp. 145–185, Springler-Verlag, Paris.

25. Evans, E. & Ritchie, K. (1997). Dynamic strength of molecular adhesion bonds. *Biophys. J.* **72**, 1541–1555.

26. Qiang, B. Q. & Schildkraut, I. (1984). A type II restriction endonuclease with an eight nucleotide specificity from *Streptomyces fimbriatus*. *Nucl. Acids Res.* **12**, 4507–4516.

27. Koch, S. J. & Wang, M. D. (2003). Dynamic force spectroscopy of protein-DNA interactions by unzipping DNA. *Phys. Rev. Letters*, **91**, 028103-1–4.

28. Eckel, R., Wilking, S. D., Becker, A., Sewald, N., Ros, R. & Anselmetti, D. (2005). Single-molecule experiments in synthetic biology: an approach to the affinity ranking of DNA-binding peptides. *Angew Chem. Int. Ed. Engl.* **44**, 3921–3924.

29. Tinoco, I, Jr & Bustamante, C. (2002). The effect of force on thermodynamics and kinetics of single molecule reactions. *Biophys. Chem.* **101-102**, 513–533.

30. Strunz, T., Oroszlan, K., Schafer, R. & Guntherodt, H. J. (1999). Dynamic force spectroscopy of single DNA molecules. *Proc. Natl Acad. Sci. USA*, **96**, 11277–11282.

31. Murphy, M. C., Rasnik, I., Cheng, W., Lohman, T. M. & Ha, T. (2004). Probing single-stranded DNA conformational flexibility using fluorescence spectroscopy. *Biophys. J.* **86**, 2530–2537.

32. Netz, R. R. & Andelman, D. (2003). Neutral and charged polymers at interfaces. *Phys. Rep.* **380**, 1–95.

33. Zhang, Y., Zhou, H. & Ou-Yang, Z. C. (2001). Stretching single-stranded DNA: interplay of electrostatic, base-pairing, and base-pair stacking interactions. *Biophys. J.* **81**, 1133–1143.

34. Ros, R., Schwesinger, F., Anselmetti, D., Kubon, M., Schafer, R., Pluckthun, A. & Tiefenauer, L. (1998). Antigen binding forces of individually addressed single-chain Fv antibody molecules. *Proc. Natl Acad. Sci. USA*, **95**, 7402–7405.

35. Yuan, C., Chen, A., Kolb, P. & Moy, V. T. (2000). Energy landscape of streptavidin-biotin complexes measured by atomic force microscopy. *Biochemistry*, **39**, 10219–10223.

36. Schlierf, M. & Rief, M. (2006). Single-molecule unfolding force distributions reveal a funnel-shaped energy landscape. *Biophys. J.* **90**, L33–L35.

37. Nevo, R., Stroh, C., Kienberger, F., Kaftan, D., Brumfeld, V., Elbaum, M. *et al.* (2003). A molecular switch between alternative conformational states in the complex of Ran and Importin Beta1. *Nature Struct. Biol.* **10**, 553–557.

38. Nevo, R., Brumfeld, V., Kapon, R., Hinterdorfer, P. & Reich, Z. (2005). Direct measurement of protein energy landscape roughness. *EMBO Rep.* **6**, 482–486.

39. Neuert, G., Albrecht, C., Pamir, E. & Gaub, H. E. (2006). Dynamic force spectroscopy of the digoxigenin-antibody complex. *FEBS Letters*, **580**, 505–509.

40. Sulchek, T. A., Friddle, R. W., Langry, K., Lau, E. Y., Albrecht, H., Ratto, T. V. *et al.* (2005). Dynamic force spectroscopy of parallel individual mucin1-antibody bonds. *Proc. Natl Acad. Sci. USA*, **102**, 16638–16643.

41. Nelson, H. C., Finch, J. T., Luisi, B. F. & Klug, A. (1987). The structure of an oligo(dA).oligo(dT) tract and its biological implications. *Nature*, **330**, 221–226.

42. Bell, G. I. (1978). Models for the specific adhesion of cells to cells. *Science*, **200**, 618–627.

Edited by A. Klug